Journal of Applied Polymer Science

Mechanical and thermal properties of low density polyethylene composites filled with dye-loaded shell powder

Wenye Yang,[1] Liuqin Ge,[1] Han Lv,[1] Meisheng Xia,[1,2] Xiaosheng Ji,[1] Zhitong Yao[3]

[1]Department of Marine Science, Ocean College, Zhejiang University, Zhoushan 316021, China

[2]State Key Laboratory of Satellite Ocean Environment Dynamics, Second Institute of Oceanography, State Oceanic Administration, Hangzhou 330100, China

[3]Department of Environment,, College of Materials Science and Environmental Engineering, Hangzhou Dianzi University, Hangzhou 310018, China

Correspondence to: X. Ji (E-mail: jixiaoshen@hotmail.com) and Z. Yao (E-mail: sxyzt@126.com)

ABSTRACT: To achieve reinforcement and coloring in one combined process of polymer production, a dye-loaded shell powder (DPSP) based on Congo red and pearl shell powder was prepared and used as a versatile bio-filler in low-density polyethylene (LDPE). The DPSP was characterized by means of X-ray diffraction, Fourier transform infrared spectroscopy and thermogravimetric analysis. The mechanical, thermal, and colorimetric properties of prepared LDPE/DPSP composites were investigated as well. Adding DPSP could significantly increase the strength and stiffness of LDPE composites while giving an outstanding coloring performance. Moreover, the impact strength of LDPE composites was improved at lower filler loading rate, and the maximum incorporation content could reach 10 wt % with a good balance between toughness and stiffness of LDPE composites. The thermal performance studies confirmed an increase in thermal stability and heat resistance of LDPE composites with the incorporation of DPSP. © 2016 Wiley Periodicals, Inc. J. Appl. Polym. Sci. **2016**, *133*, 44118.

KEYWORDS: biomaterials; composites; dyes/pigments; mechanical properties; thermal properties

Received 28 January 2016; accepted 23 June 2016

DOI: 10.1002/app.44118

INTRODUCTION

An improvement in the mechanical–physical properties of polymeric materials, with a simultaneous giving color, can be obtained by the use of a kind of hybrid pigment obtained from a combination of organic dyes and inorganic mineral. In the past few years, a type of nanoclay-based pigment (NCP) obtained from clay modified with soluble dyes was synthesized and applied to different polymers.[1–5] Fischern and Fischern *et al.*[6,7] claimed that these NCPs benefitted from the advantages of dyes, such as bright colors and a wide color gamut and avoided their drawbacks, such as low lightfastness and low stability against temperature due to the barrier action of exfoliated clay particles. Marchante *et al.*[8] prepared several blue NCPs with Na-montmorillonite and methylene blue (MB), and found that the PE/NCP composites showed better color properties than those containing conventional colorants. In addition, the presence of NCPs could increase the mechanical properties of PE/NCP samples, but did not noticeably affect their thermal stability. Beltrán *et al.*[9] synthesized organomontmorillonites (OMt) combing different proportions of MB and ethyl hexadecyl dimethyl ammonium, then mixed OMt with ethylene vinyl acetate (EVA) copolymer. All the colored EVA/OMt composites showed an increase in the Young's modulus compared to the EVA reference. Combining the advantages of dye coloration and nanoclay filling, these additives can improve the mechanical–physical properties of polymers while giving good color performance. Nevertheless, clay minerals are hydrophilic in nature, and even after modification, are difficult to disperse into a polymer matrix, which limits the filler content and thus the color gamut. In those previous reports,[5,8–10] the Young's modulus of polymer/NCP composites were improved, however, some mechanical properties like tensile strength and impact strength were not noticeably enhanced or even decreased as NCPs content increased. With respect to the thermal behaviors, samples of the polymer/NCP composites did not show significant modification in thermal stability, regardless of fillers loading. Although the reinforcement effects of this additive are not so satisfactory, it provides a novel method for polymer reinforcement and coloring. Therefore, there is a potential to develop an inorganic substrate for dyes, which can significantly improve the mechanical–physical properties of polymers while giving an outstanding color performance with low cost and simple process.

Shellfish shell as a natural biocomposite consists about 95% calcium carbonate ($CaCO_3$) and a small amount of organic

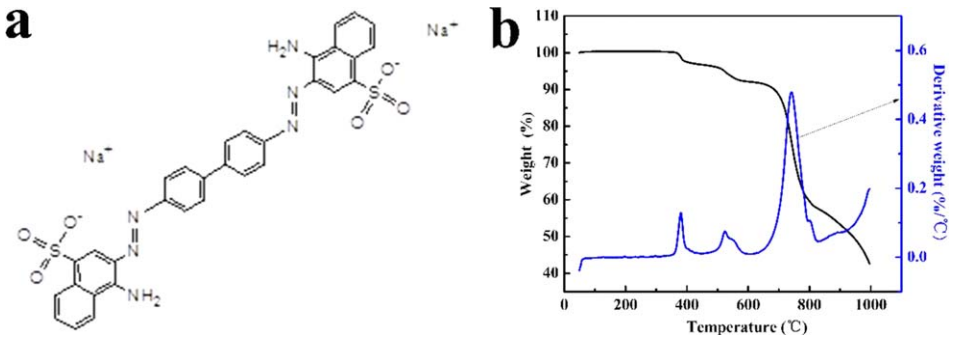

Figure 1. Chemical structure (a) and TGA/DTG curves (b) of CR. [Color figure can be viewed in the online issue, which is available at wileyonlinelibrary.com.]

materials, such as glycoproteins, polysaccharides, glycosaminoglycan, chitin, and other proteins.[11,12] Nacre is arranged in brick-mortar microstructure with organic sheets in the inner layer of the shell and exhibits an excellent mechanical properties.[13–15] Jackson *et al.*[16] investigated the nacre from Pinctada shell and reported a Young's modulus of 70 GPa, and tensile strength of 170 MPa for dry samples. In contrast, monolithic $CaCO_3$ showed a work-of-fracture approximately 3000 times less than that of the composite nacre material.[17] Meyers *et al.*[18] concluded that shell had a lower density as well as a larger surface area, and it was cost-reducing and environ mentally friendly, as compared with mineral $CaCO_3$. Moreover, the organic matrices in shell can be fully exposed via pulverizing and grinding repeatedly during the preparation, making the powder of shell more easily dispersed into organic polymer than inorganic mineral $CaCO_3$, based on the "like dissolve like" rule. Li *et al.*[19] prepared polypropylene (PP) composites with Mytilus edulis powder and reported a higher yield strain, yield strength, tensile strength and elongation at break point, as compared with commercial $CaCO_3$. Yao *et al.*[20–22] confirmed that the incorporation of organically modified clam shell powder played a toughening and reinforcing role in PP composites. Lin *et al.*[23] investigated the scallop shell/PP composites and found that the inclusion of pimelic acid modified shell powder greatly increased the impact strength of PP.

In this work, we attempted to combine the advantages of hybrid pigment coloring and shell powder reinforcement to prepare a dye-loaded shell powder (DPSP) based on pearl shell powder (PSP) and Congo red (CR) dye. It was characterized by means of X-ray diffraction (XRD), Fourier transform infrared spectroscopy (FTIR), and thermogravimetric analysis (TGA) and then incorporated into low-density polyethylene (LDPE) with a wide range of content (2–40 wt %). The mechanical, thermal, and colorimetric properties of LDPE composites were investigated as well.

EXPERIMENTAL

Materials

Commercial grade LDPE (2426H) with a melt flow index of 1.9 g/10 min at 190 °C was provided by Sinopec Maoming Company (Guangdong, China). PSP was obtained by a food factory in Tianjin, China. Organic CR (C.I. 22120) was supplied by Yiwu Yufang Pigment Commercial Firm (Yiwu, China). Processing agent: mineral oil, maleic anhydride grafted polyethylene (PE-g-MAH), antioxidant 168 and lubricant were all provided by Xingtaiguoguang Chemical Additives Co., Ltd (Suzhou, China).

CR is an azo and anionic dye [Figure 1(a)]. The dye is water-soluble because of the sulfonic acid group (SO_3^-) on its naphthalene nuclei, simplifying the dyeing process. The presence of azo (–N═N–) groups and rich aromatic rings impart a good thermal stability to the dye. As can be seen from the TGA/DTG curves of CR [Figure 1(b)], the onset degradation temperature is about 380.8 °C, higher than the processing temperature of most plastics.

Preparation of DPSP

An amount of 10 g of CR was dispersed in 3 L of deionized water under magnetic stirring for 0.5 h at 40 °C to make the CR dissolved in water adequately. After that, the raw PSP at a PSP-to-dye mass ratio of 200:1 was slowly added to the dye solution with vigorous stirring maintained for 1 h. The formed slurry was left for lasting 24 h to reach the adsorption equilibrium of CR, and then, filtered and washed out repeatedly until the color floating was removed. Finally, the filter residue was dried and grinded for obtaining the colored DPSP. The particle size of DPSP was smaller than that of PSP due to the secondary pulverization during DPSP preparation. Approximately, 75% of the DPSP was less than 2 μm in diameter, 90% less than 3 μm, and 97% less than 5 μm, measured by a Coulter LS-230 laser particle size analyzer.

Preparation of the LDPE Composites

LDPE pellets and DPSP with the weight contents of 0, 2, 5, 10, 15, 20, 30, and 40% were melt-mixed individually using a Berstorff SHJ-35 twin-screw extruder (Quanta chemical equipment co., LTD, China) with a screw diameter of 35 mm and *L*/*D* ratio of 52:1 at a screw speed of 75 rpm. The barrel temperatures of extruder set at 225/220/220/210/205/205/205/220/220/205/215/220 °C from the feed zone to the extruder head. To improve mixing, DPSP and virgin LDPE particles were dried in a 101A-4B vacuum oven (Hangzhou ZhuoChi instrument co., LTD, China) at 80 °C for 4 h, and pre-mixed with 5 wt % PE-g-MAH, 1.5 wt % lubricant, 0.1 wt % antioxidant 168, and 0.1 wt % mineral oil using a SHR-25A high-speed mixer (Jinfeng Shenma Plastic machinery factory, Zhangjiagang, China). The extrusion process was carried out in a continuous manner, and obtained composites were immediately cooled by water and

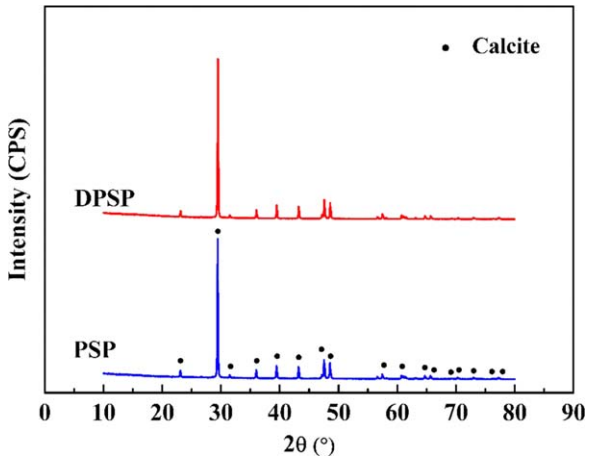

Figure 2. XRD patterns of PSP and DPSP. [Color figure can be viewed in the online issue, which is available at wileyonlinelibrary.com.]

pelletized into granule. A MA 900/260 injection-molding machine (Haitian Plastic machinery group Co., Ltd, China) was used for preparing the standard samples for the subsequent tests. The injection temperatures set at 185/200/200/180/165 °C from the first to the fifth segment.

Characterization and Tests

The composition of PSP and DPSP was identified by the Japanese Rigaku D-max/IIB X-ray power diffractometer: Cu Kα radiation (λ = 0.154068 nm), acceleration voltage of 40 kV, step size of 0.01° and a range of 10°–80°on the 2θ scale. Infrared spectra were recorded over 400 to 4000 cm^{-1} region on a Nicolet NEXUS 670 Fourier Transform Infrared Spectrometer Instrumentation by KBr pellet pressing method at room temperature. TGA–differential thermal gravity (DTG) analysis from 50 to 1000 °C was carried out on a Pyris Diamond TG-Q500 thermal gravimetric analyzer at a heating rate of 10 °C/min in nitrogen atmosphere. Samples were pre-heated to 100 °C for 5 min to remove residual water.

Tensile and flexural tests were conducted on a CMT 4204 microcomputer-controlled electron universal testing machine. Notched Izod impact tests were conducted with a ZBC7151-B pendulum impact tester. All the mechanical tests were operated according to the ASTM standard method at a temperature of 23 ± 2 °C and relative humidity of 32 ± 5%. At least five specimens of each sample were tested and their mean values and standard deviations were calculated. Fracture surfaces of the test specimens were observed by scanning electron microscopy (SEM) in a Hitachi SU8000 field emission SEM at a voltage of 3 kV. All specimens were obtained at liquid nitrogen temperature and sputter-coated with platinum on the sections. The Vicat softening temperature (VST) of LDPE composites were determined by a ZWK1302-B Vicat softening point tester at a heating rate of 50 °C/h and load of 10.0 N according to the GB/*T* 1633–2000 standard. To assess the coloring performance of LDPE composites filled with the DPSP, the chrominance and luminance of samples were measured with a portable NH310 colorimeter.

RESULTS AND DISCUSSION

Characterization of PSP and DPSP

XRD Analysis. The XRD patterns of PSP and DPSP are displayed in Figure 2. It can be observed that the diffraction peaks in the diffractogram of PSP are well correspond with calcite ($CaCO_3$, JCPDS Card No. 86-2334) pattern,[24] suggesting that calcite is the major crystalline phases of PSP. The sets of characteristic peaks of PSP are also observed in DPSP pattern. Moreover, after CR modification, the XRD patterns of DPSP shows characteristic peaks similar to those of PSP, which means that the phases of PSP remain intact. The natural and especial phases of shell powder are the primary reason for the excellent mechanical properties and reinforcement effect of DPSP.

FTIR Spectra. The FTIR spectra of PSP, DPSP and CR in Figure 3 exhibit the following absorption bands and they are assigned referring to the literatures.[25–29] In the spectrum of PSP, the bands located at 711.87, 876.31, and 1420.02 cm^{-1} are ascribed to the in-plane bending, out-of-plane bending, and asymmetric stretch vibrations of CO_3^{2-} groups, respectively.[30–32] The band located at 1798.36 cm^{-1} is assigned to the combination of C=O stretching vibration and –NH– in-plane bending vibration. The band at 2512.90 cm^{-1} is provided by HCO_3^-. The bands of C–H stretching (2873.36 and 2981.46 cm^{-1}), and –OH or $–NH_2$ stretching (3401.87 cm^{-1}) are confirmed. The presence of N and organic carbon functional groups reveals the presence of organic matrix in shell powder, which is also the base of organic modification for PSP.

For CR, the bands at 617.30 and 752.78 cm^{-1} are the out-of-plane bending vibration of C-H on aromatic nuclei. The band at 831.96 cm^{-1} is due to the p-disubstituted ring vibrations, and the band at 1124.84 cm^{-1} is attributable to the stretching vibration of S=O stretching vibrations of SO_3^-. The band at 1363.97 cm^{-1} is due to bending vibrations of C–N, 1446.66 cm^{-1} for (C=C) aromatic stretching vibrations, and 1583.09 cm^{-1} for N=N stretching vibrations. The characteristic absorption band of $—NH_2$ (3465.80 cm^{-1}) is conformed, which can form hydrogen bonds with the amino groups on

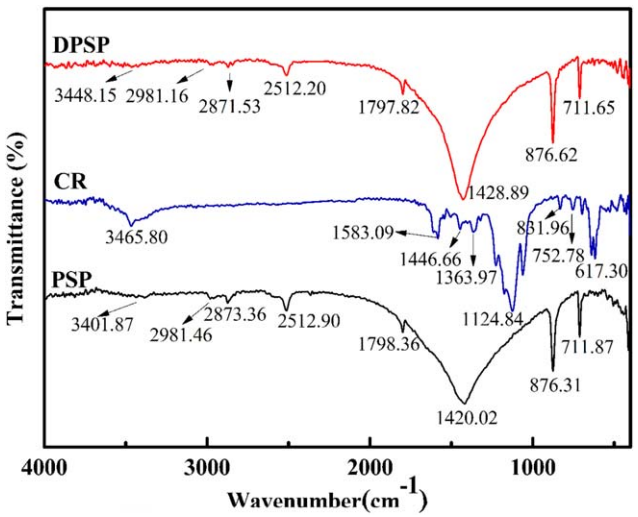

Figure 3. FTIR spectra of PSP, DPSP and CR. [Color figure can be viewed in the online issue, which is available at wileyonlinelibrary.com.]

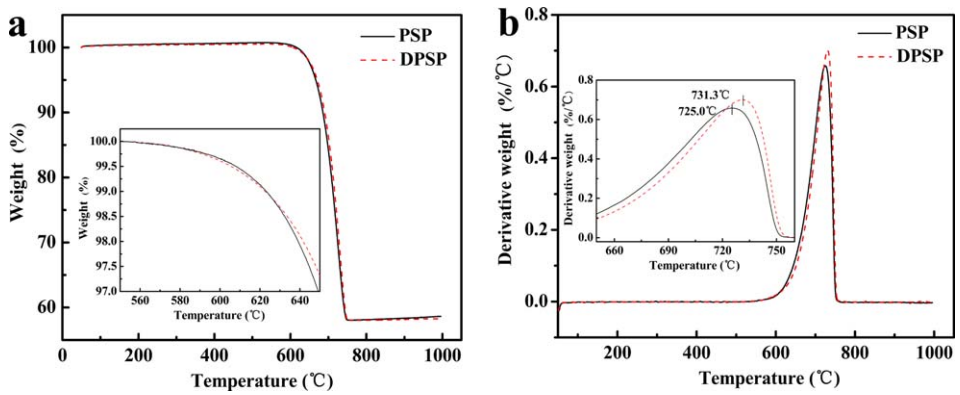

Figure 4. TGA (a) and DTG (b) curves of PSP and DPSP. [Color figure can be viewed in the online issue, which is available at wileyonlinelibrary.com.]

PSP. As the amount of dye adsorbed on PSP is quite small (less than 0.5 wt %), the spectrum of DPSP shows characteristic bands similar to that of PSP. However, the relatively obvious shift from 1420.02 to 1428.89 cm^{-1} observed for the DPSP spectrum, indicating an environmental change around the CO_3^{2-} groups. In addition, the decrease of the weak band at 3401.87 cm^{-1} corresponding to $-NH_2$ is observed after CR loaded. These results can be attributed to the formation of hydrogen bond and Van der Waals force between PSP and CR.

TGA/DTG Analysis. The thermal stability of PSP and DPSP has been evaluated by means of analysis of the TGA and DTG curves in Figure 4. The TGA/DTG curves of the two specimens exhibit a barely detectable weight loss below 550 °C, which are related to the great thermal stability of the organic component and organic-mineral bonding. Furthermore, the onset decomposition temperature of calcite (550 °C) in PSP is higher than that of the nature calcite at about 420 °C, which is probably due to the influence of strong interaction between the organic and the mineral phases.[33] The sharp decomposition of PSP occurs in a single event from 550 to 750 °C corresponding to a total mass loss of approximately 41.187%, which is attributed to calcite decomposes into calcium oxide and carbon dioxide in this temperature range. Due to a part of CR loaded on the PSP begin to decompose at a relatively low temperature, the strong decomposition temperature of DPSP at about 731.3 °C is higher than that of PSP, while the total mass loss increase to 42.875%. Because of the great thermal stability of the DPSP, it can be used as a kind of versatile bio-filler to blend with LDPE at about 220 °C.

Characterization of LDPE Composites

Mechanical Properties. Mechanical properties of LDPE composites are displayed in Figure 5. It can be seen that the tensile strength and flexural strength both increased significantly with increasing the DPSP content. Compared to that of neat LDPE, when 40 wt % content of DPSP was incorporated, the tensile strength increased from 12.20 to 14.13 MPa, and the flexural strength from 10.48 to 19.80 MPa—increases of 15.82% and 88.93%, respectively. These results are ascribed to the good filler dispersity and strong interfacial bonding, which can be confirmed through the SEM photograph on the fracture surfaces of test bars showed in Figure 6. The addition of filler particles bond with the molecular chains of LDPE matrix borne fraction of the external tensile load, and tensile stress transferred from the matrix along the fillers giving rise to effective and uniform stress distribution. Therefore, the two strength properties are largely enhanced with an increasing amount of DPSP added.

Dissimilar to the trend recorded in the tensile strength and flexural strength, there was an overall decrease in the elongation at break point for LDPE composites filled with DPSP. It significantly decreased from 171.60 to 75.20%, as the filler content increased to 40 wt %. The decrement in elongation at break point with increasing filler content is due to the incorporation of rigid filler particles restricted the relative movement of the polymer molecules, which is characteristic of reinforced thermoplastic composites.[34] When the low elongation of DPSP were added into LDPE matrix, the specimens became stiffer. As expected, the tensile modulus and flexural modulus representing stiffness of material increased almost linearly with the rise of the filler level.

As for the impact strength, when the filler content was lower than a critical value of 5 wt %, the impact strength increased with filler content increase; when the loading rate was higher than 5 wt %, the impact strength decreased again. The impact strength increased to 69.52 KJ/m^2 with an incorporation of 5 wt %, and it did not lower than that of neat LDPE (65.33 KJ/m^2) until the filler content was larger than 10 wt %. The increase in the filler content results in the decrease in the polymer matrix content in the composites. For small amounts, the filler which dispersed in LDPE matrix uniformly can absorb part of the energy and reduce a predominantly shear yielding mechanism of failure without damaging the overall continuous thermoplastic phase of LDPE.[35] However, for higher amounts of filler, its dispersion in LDPE matrix became difficult. The impact load could lead to a physical separation between the filler and the matrix. The debonded particles bore no fraction of the external load, consequently the impact strength decreased. In addition, the agglomerates tend to create weak points in the matrix because of stress concentration effect, thereby triggering a crack initiation which is extremely sensitive for the toughness of the composite.[36–38]

The mechanical properties studies showed that adding DPSP could significantly increase the tensile strength, flexural strength, tensile modulus, and flexural modulus of LDPE composites. Moreover, the impact strength of LDPE composites was improved at lower filler loading rate. Therefore, the inclusion of

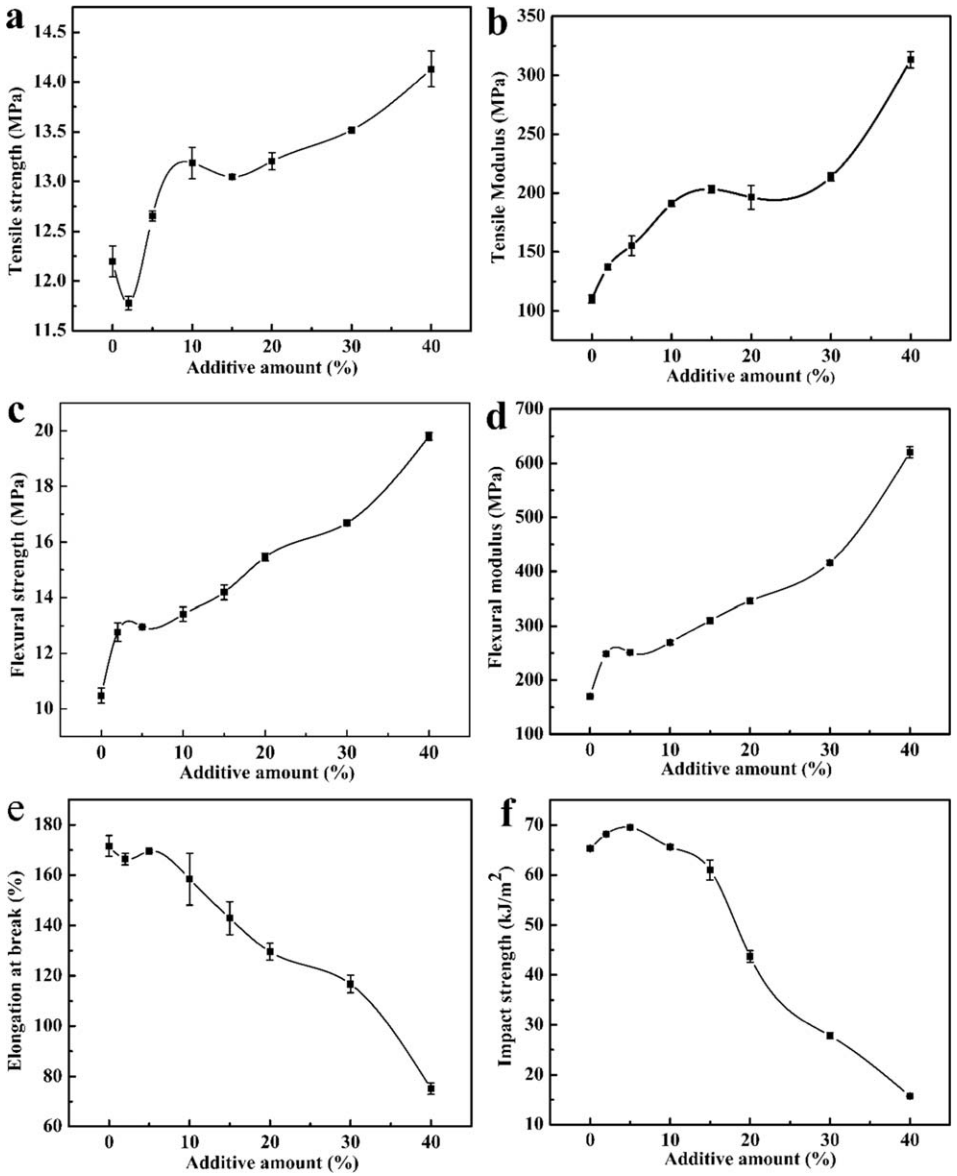

Figure 5. Mechanical properties of neat LDPE and LDPE composites.

DPSP played a reinforcing and toughening role in LDPE composites, although its toughening effect was not significant. Obviously, the maximum incorporation content could reach 10 wt % with a good balance between toughness and stiffness of LDPE composites.

TGA/DTG Analysis. Thermal stability of neat LDPE and LDPE composites are presented in Figure 7. As is shown, all of the composites have a similar one-step decomposition pattern occurring at approximately 380–510 °C, which correspond to the degradation of LDPE backbone. The maximum degradation rate of all the LDPE composites located at around of 480 °C. Those similar decomposition behavior indicate that the presence of DPSP did not significantly influence the thermal-degradation pattern of LDPE composite. However, the thermal-decomposition temperatures (T 50%) and the residue weight (the residue percent at 550 °C increased from 1.324 (for net LDPE) to 43.177% for compositions with 40 wt % of DPSP) apparently increased, especially at higher filler contents, indicating improvement in the thermal stability of the LDPE matrix from incorporation of DPSP. Therefore, increase in the DPSP filler component in composites could inhibit the LDPE matrix decomposition and thus improved the thermal stability of LDPE composites.

VST Test. VST tests are measured to determine the heat softening characteristics of LDPE composites. The VST for neat LDPE and LDPE composites with various DPSP contents were measured and showed in Figure 8. As can be seen, the VST representing heat resistance of LDPE composites were improved significantly by adding fillers. When the 40 wt % filler was incorporated, the VST of LDPE composites increased from 94 °C (net LDPE) to 98.7 °C. The presence of fillers improved the heat resistance characteristics of LDPE composites for their

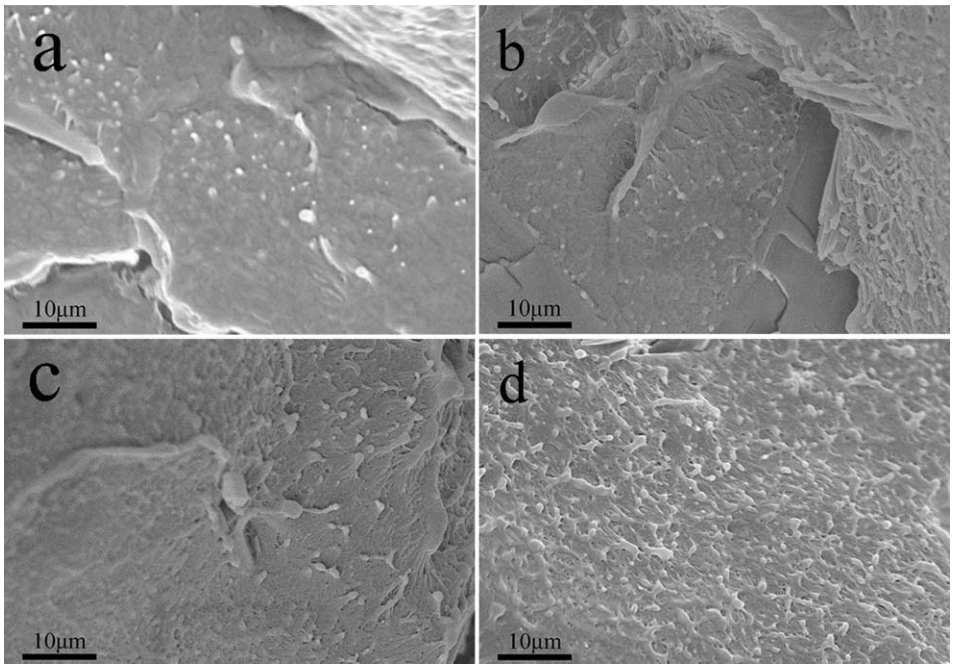

Figure 6. SEM images of the specimen sections with different filler content: (a) 5%; (b) 15%; (c) 30%; (d) 40%.

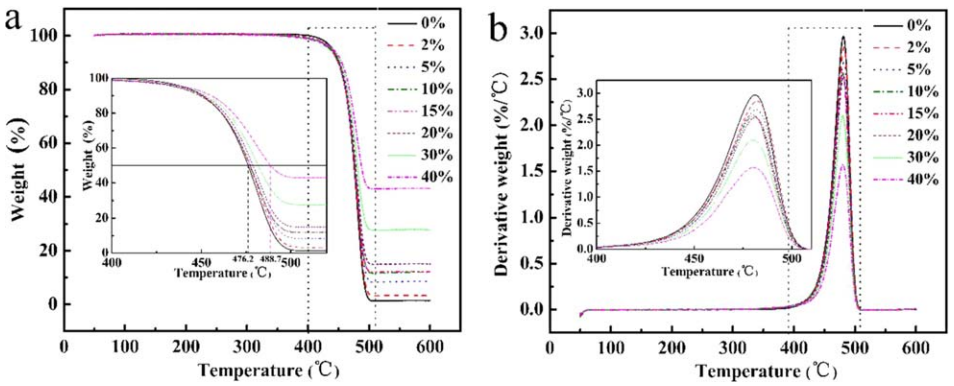

Figure 7. TGA (a) and DTG (b) curves of neat LDPE and LDPE composites. [Color figure can be viewed in the online issue, which is available at wileyonlinelibrary.com.]

potential practical application in an elevated temperature. The increase of the VST of LDPE composites mainly due to the increase in the stiffness of composites and the presence of DPSP particles within the composites. The presence of DPSP particles limited the movement of the whole macromolecular chains, thereby, prevented the elastic and plastic deformation of LDPE composites.[39,40] In addition, the improvement of heat resistance may also be attributed to the low thermal conductivity of DPSP fillers with the main component of calcite.[41]

Colorimetric Analysis. The Chromatic (L^*, a^*, b^*) of LDPE composites was measured by CIE-$L^*a^*b^*$ color system coordinates and the color differences ($\triangle E^*_{ab}$, $\triangle L^*$, $\triangle a^*$, and $\triangle b^*$) between LDPE composites and neat LDPE were calculated. The L^* representing the brightness or darkness of the color is positively correlated with lightness. The a^* and b^* indexes quantify chromaticity, and the values from positive to negative reflect the color shifting from red to green, blueness to yellowness,

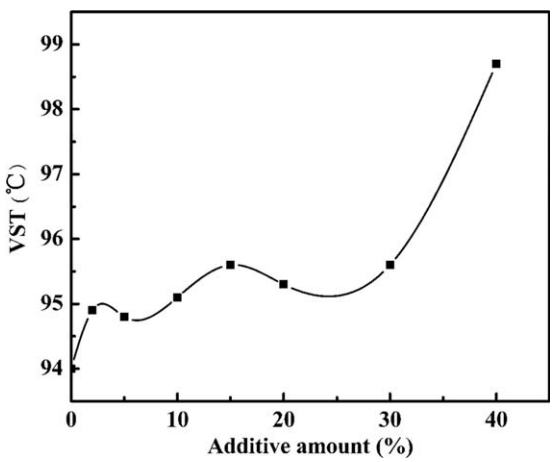

Figure 8. VST of net LDPE and LDPE composites.

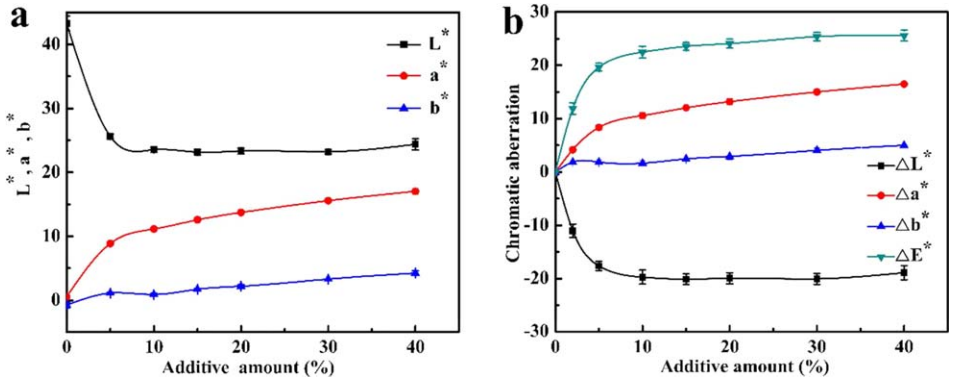

Figure 9. Chromatic diagram (a) and Color differences (b) of net LDPE and LDPE composites. [Color figure can be viewed in the online issue, which is available at wileyonlinelibrary.com.]

respectively. $\triangle L^{\star}$, $\triangle a^{\star}$, and $\triangle b^{\star}$ represent the differences in lightening, the red–green component, and the yellow–blue component, respectively. $\triangle E^{*}_{ab}$ represents the total color difference.

Here, the several types of color differences are calculated by the following equations (subscript "0" represents neat LDPE):

$$\triangle L^{*} = L^{*} - L^{*}_{0} \quad (1)$$

$$\triangle a^{*} = a^{*} - a^{*}_{0} \quad (2)$$

$$\triangle b^{*} = b^{*} - b^{*}_{0} \quad (3)$$

$$\triangle E^{*} = \sqrt{\triangle L^{*2} + \triangle a^{*2} + \triangle b^{*2}} \quad (4)$$

The Chromatic diagram and color differences of the LDPE composites with various filler contents are presented in Figure 9. The values of $L^{\star}$ decreased significantly until the filler content was more than 10 wt %, and the values of $\triangle L^{\star}$ were negative, indicating that some absorbance of the incident light due to the presence of the PSP.[42] The values of $b^{\star}$ and $\triangle b^{\star}$ changed slightly, whereas the values of $a^{\star}$ and $\triangle a^{\star}$ keep increasing apparently and they are both positive, signifying the color of LDPE composites shift toward red notably as the filler level rose. As to the total color difference ($\triangle E^{\star}$), it is clearly that $\triangle E^{\star}$ increased when the filler content was lower than 10 wt %. However, when the filler content was much larger, there was no further pronounced changes in $\triangle E^{\star}$ with the addition of more DPSP. The variation trend of $\triangle E^{\star}$ is mainly resulted from the changes of $\triangle a^{\star}$ and $\triangle L^{\star}$ with positive and negative values, respectively. This means that the color of the LDPE composites shifted to red and dark with increasing filler content. Furthermore, the appearance of whole set samples showed a uniform distributions of color, which could be ascribed to the good dispersity of DPSP in the LDPE matrix. In fact, the absorbed dye bestowed color and acted as surfactant for the PSP, making the filler more compatible with the polymer matrix and giving color to LDPE composites. The color of LDPE composites did not reach saturation until 10 wt % of DPSP was filled; therefore, a wide color gamut of LDPE composites could be obtained. These results demonstrated that the dyeing process with DPSP is successful.

CONCLUSIONS

In this work, one kind of versatile bio-filler DPSP benefited from the advantage of organic dye and shellfish shell powder was prepared and melt-mixed with LDPE. Due to the well-dispersed filler can bore fraction of the external load, LDPE composites showed a good coloring performance and a significant promotion in the strength. The DPSP particles within the composites restricted the relative movement of the polymer molecules and caused a remarkable increase in the tensile modulus and the flexural modulus of LDPE composites. Furthermore, the filler had a toughening effect at low filler concentrations and the maximum incorporation content could reach 10 wt % with a good balance between stiffness and toughness of LDPE composites. The thermal stability and heat resistance of LDPE composites also increased with increasing the filler content. Therefore, with only one additive it is successful to derive two important benefits, namely improving the mechanical–physical properties of the polymers while adding color.

ACKNOWLEDGMENTS

This work was supported by National Science Foundation of China (529101). We would also like to thank Hangzhou HONYAR Electrical Co., LTD, China for the assistance of plastic processing and testing.

REFERENCES

1. Fischer,H. R.; Gielgens,L. H.; Koster,T. In Materials Research Society Symposium Proceedings; Laine, R. M.; Sanchez, C.; Brinker, C. J.; Giannelis, E., Eds.; Materials Research Society: Warrendale, **1998**; Vol. *519*, Chapter Organic/Inorganic Hybrid Materials, p 117.
2. Ataeefard, M.; Moradian, S. *J. Appl. Polym. Sci.* **2012**, *1251*, E214.
3. Raha, S.; Ivanov, I.; Quazi, N. H.; Bhattacharya, S. N. *Appl. Clay Sci.* **2009**, *42*, 661.
4. Volle, N.; Challier, L.; Burr, A.; Giulieri, F.; Pagnotta, S.; Chaze, A. *Compos. Sci. Technol.* **2011**, *71*, 1685.
5. Marchante Rodriguez, V.; Martinez-Verdu, F. M.; Beltran Rico, M. I.; Marcilla Gomis, A. *Pigm. Resin Technol.* **2012**, *41*, 263.
6. Fischer, H. *Mat. Sci. Eng. C* **2003**, *23*, 763.

7. Fischer, H. R.; Gielgens, L. H.; Koster, T. *Acta Polym.* **1999**, *50*, 122.
8. Marchante, V.; Marcilla, A.; Benavente, V.; Martinez-Verdu, F. M.; Beltran, M. I. *J. Appl. Polym. Sci.* **2013**, *129*, 2716.
9. Beltran, M. I.; Benavente, V.; Marchante, V.; Dema, H.; Marcilla, A. *Appl. Clay Sci.* **2014**, *97–98*, 43.
10. Marchante, V.; Benavente, V.; Marcilla, A.; Miguel Martinez-Verdu, F.; Isabel Beltran, M. *J. Appl. Polym. Sci.* **2013**, *130*, 2987.
11. Marin, F.; Luquet, G. *Mat. Sci. Eng. C* **2005**, *25*, 105.
12. Sudo, S.; Fujikawa, T.; Nagakura, T.; Ohkubo, T.; Sakaguchi, K.; Tanaka, M.; Nakashima, K.; Takahashi, T. *Nature* **1997**, *387*, 563.
13. Katti, K. S.; Katti, D. R. *Mat. Sci. Eng. C* **2006**, *26*, 1317.
14. Grujicic, M.; Snipes, J. S.; Ramaswami, S. *J. Mater. Eng. Perform.* **2016**, *25*, 977.
15. Heinemann, F.; Launspach, M.; Gries, K.; Fritz, M. *Biophys. Chem.* **2011**, *153*, 126.
16. Jackson, A. P.; Vincent, J.; Turner, R. M. *Proc. Biol. Sci.* **1988**, *234*, 415.
17. Currey, J. D.; Zioupos, P.; Davies, P.; Casinos, A. *Proc. Biol. Sci.* **2001**, *268*, 107.
18. Meyers, M. A.; Lin, A. Y.; Chen, P.; Muyco, J. *Mech. Behav. Biomed. Mater.* **2008**, *1*, 76.
19. Li, H.; Tan, Y.; Zhang, L.; Zhang, Y.; Song, Y.; Ye, Y.; Xia, M. *J. Hazard. Mater.* **2012**, *217–218*, 256.
20. Yao, Z.; Xia, M.; Ge, L.; Chen, T.; Li, H.; Ye, Y.; Zheng, H. *Fiber Polym.* **2014**, *15*, 1278.
21. Yao, Z. T.; Chen, T.; Li, H. Y.; Xia, M. S.; Ye, Y.; Zheng, H. *J. Hazard. Mater.* **2013**, *262*, 212.
22. Yao, Z.; Ge, L.; Ji, X.; Tang, J.; Xia, M.; Xi, Y. *J. Alloy. Compd.* **2014**, *621*, 389.
23. Lin, Z.; Guan, Z.; Chen, C.; Cao, L.; Wang, Y.; Gao, S.; Xu, B.; Li, W. *Thermochim. Acta* **2013**, *551*, 149.
24. Ramasamy, V.; Suresh, G.; Meenakshisundaram, V.; Ponnusamy, V. *Appl. Radiat. Isot.* **2011**, *69*, 184.
25. Szumera, M. *Spectrochim. Acta A* **2014**, *130*, 1.
26. Katmiwati, E.; Nakanishi, T. *Macromol. Res.* **2014**, *22*, 731.
27. Meng, F.; Tahmasebi, A.; Yu, J.; Zhao, H.; Han, Y.; Lucas, J.; Wall, T. *Energy Fuel* **2014**, *28*, 5612.
28. Kashyout, A.; Soliman, H.; Nabil, M.; Bishara, A. *Sens. Actuators B* **2015**, *216*, 279.
29. Mota, T. R.; Kato, C. G.; Peralta, R. A.; Bracht, A.; de Morais, G. R.; Baesso, M. L.; Marques De Souza, C. G.; Peralta, R. M. *Water Air Soil Pollut.* **2015**, *226*,
30. Cifrulak, S. D. *Am. Mineral.* **1970**, *55*, 815.
31. Kamba, A. S.; Ismail, M.; Ibrahim, T. A. T.; Zakaria, Z. A. B. *J. Nanomater.* **2013**, *107*, 268.
32. Zhu, J.; Song, J.; Yu, S.; Zhang, W.; Shi, J. *CrystEngComm* **2009**, *11*, 539.
33. Balmain, J.; Hannoyer, B.; Lopez, E. *J. Biomed. Mater. Res. A* **1999**, *48*, 749.
34. Xia, M.; Yao, Z.; Ge, L.; Chen, T.; Li, H. *J. Compos. Mater.* **2015**, *49*, 807.
35. Lima, P. S.; Oliveira, J. M.; Ferreira Costa, V. A. *J. Appl. Polym. Sci.* **2015**, *132*, DOI: 10.1002/app.42011.
36. Yao, Z.; Ge, L.; Ji, X.; Tang, J.; Xia, M.; Xi, Y. *J. Alloy. Compd.* **2015**, *621*, 389.
37. Fu, S.; Feng, X.; Lauke, B.; Mai, Y. *Compos. Part B* **2008**, *39*, 933.
38. Hartikainen, J.; Hine, P.; Szabo, J. S.; Lindner, M.; Harmia, T.; Duckett, R. A.; Friedrich, K. *Compos. Sci. Technol.* **2005**, *65*, 257.
39. Zhang, Y.; Yu, C.; Chu, P. K.; Lv, F.; Zhang, C.; Ji, J.; Zhang, R.; Wang, H. *Mater. Chem. Phys.* **2012**, *133*, 845.
40. Chen, W.; Pang, M.; Xiao, M.; Wang, S.; Wen, L.; Meng, Y. *J. Reinf. Plast. Compos.* **2010**, *29*, 1545.
41. Zheng, Y.; Shen, Z.; Cai, C.; Ma, S.; Xing, Y. *J. Hazard. Mater.* **2009**, *163*, 600.
42. Raha, S.; Quazi, N.; Ivanov, I.; Bhattacharya, S. *Dyes Pigm.* **2012**, *93*, 1512.